Journal of Micromechanics and Microengineering

Highlights of 2015

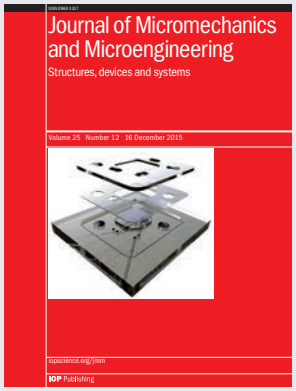

Did you know?
JMM articles received more than **425,000** full-text article downloads in 2015

Dear Colleagues,

As the publisher of *Journal of Micromechanics and Microengineering* (JMM), I am delighted to present the journal Highlights of 2015. These are intended as a showcase for the exciting research across all areas of MEMS and microscale research that JMM publishes. All the Highlights are free to read until the end of 2016.

The chosen articles were identified by our team of expert referees and the journal's Editorial Board as some of the highest-quality papers we have published in 2015. I hope that you find them interesting.

To find out more about *Journal of Micromechanics and Microengineering* and to read the full-text versions, please go to **iopscience.org/jmm**.

Ian Forbes
Publisher, *Journal of Micromechanics and Microengineering*

Great science deserves great recognition

On-chip high density droplet-on-template (DOT) array

Jitae Kim and Simon Song

Abstract

In this report, we present a new method for generating a high-density (2D) droplet array using double-layered polydimethylsiloxane (PDMS) templates containing honeycomb microwells. Without external flow control, a droplet-on-template (DOT) was created by utilizing capillary forces associated with the interfacial tension between the aqueous and oil phases. The DOT process involved three simple steps: (1) vacuum-assisted filling of microwells; (2) excess water removal; and (3) covering the droplet array with oil. To demonstrate the concept of the DOT, we generated spherical water droplets 147, 191, 238, 326 and 405 μm in diameter from corresponding microwells with lengths of 200, 300, 400, 600 and 800 μm, respectively and a height of 76 μm (up to ~10,000 droplets on a template 25 × 25 mm). Two important factors, including the aspect ratio (height-to-length ratio) of the microwell and the interfacial tension of the two phases, were investigated to understand how those factors affect the shape of the droplets ('sphere' or 'dome'). All the droplets were spherical up to an aspect ratio of 0.55. The droplets were dome-shaped for aspect ratios above 0.82. For a 1 mM sodium dodecyl sulfate (SDS) solution, the use of mineral oil (which had the highest interfacial tension studied) produced spherical droplets, but dome-shaped droplets were produced by corn oil and oleic acid.

2015 *J. Micromech. Microeng.* **25** 017001

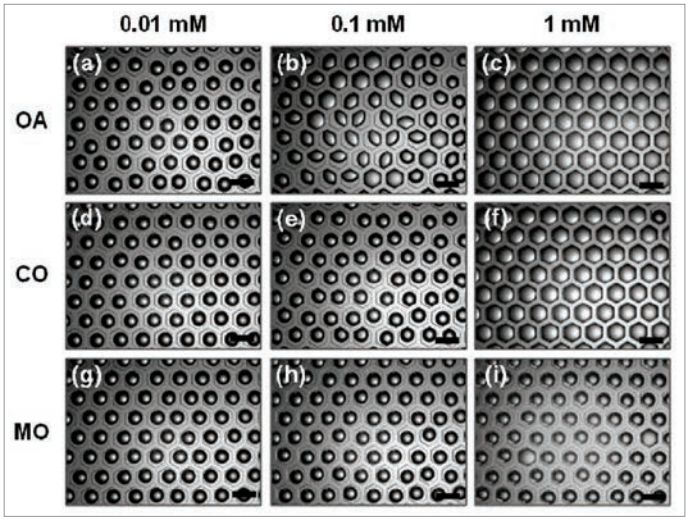

Droplet-on-template patterns formed with different oils and concentrations.

Did you know?
The average time between receipt and acceptance in 2015 was **88 days** (less than three months). Visit **iopscience.org/jmm** for more information.

Solvent-transfer assisted photolithography of high-density and high-aspect-ratio superhydrophobic micropillar arrays

Shaolin Zhou, Mingjun Hu, Qiuquan Guo, Xiaobing Cai, Xiangmin Xu and Jun Yang

Abstract

An effective and facile route of solvent-transfer assisted photolithography (STAP) was explored to successfully fabricate uprightly standing high-density (HD) and high-aspect-ratio (HAR) micropillar arrays with excellent superhydrophobicity. The collapse problem that frequently occurs with the HAR micro or nano-structures was simply resolved by the combined optimization of an SU-8 UV photolithographic process that aimed to maximize the stiffness of HAR pillars and minimize the capillary effect by fully optimizing UV exposure, resist baking and the final step of rinse and drying. The SU-8 micropillar array with high density close to 29% and varied aspect ratio up to 13:1 can be fabricated in an equivalently effective but less time-consuming and simpler way compared to conventional techniques of supercritical point drying and freeze drying. As a result, the SU-8 surfaces structured with the upright standing HD and HAR micropillars created by the combined optimization of the STAP process were demonstrated to be of superhydrophobicity with a contact angle up to 162° and those pillars array with varied AR above 5:1 assumed a slightly varied level of superhydrophobicity.

2015 *J. Micromech. Microeng.* **25** 025005

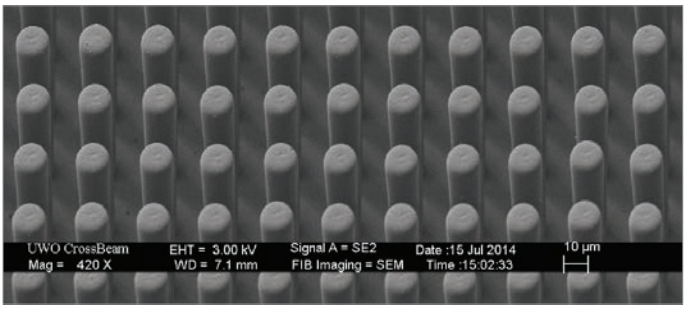

HAR superhydrophobic SU-8 micropillar array.

Manufacturing and characterization of a ceramic microcombustor with integrated oxygen storage and release element

Z Khaji, P Sturesson, L Klintberg, K Hjort and G Thornell

Abstract

A microscale ceramic high-temperature combustor with a built-in temperature sensor and source of oxygen has been designed, manufactured and characterized. The successful *in situ* electroplating and oxidation of copper, and the use of copper oxide as the source of oxygen were demonstrated. It was shown that residual stresses from electroplating, copper oxidation and oxide decomposition did not cause much deformation of the substrate but influenced mainly the integrity and adhesion of the metal films. The process had influence on the electrical resistances, however. Calibration of the temperature sensor and correlation with IR thermography up to 1000 °C revealed a nearly linear sensor behavior. Demonstration of combustion in a vacuum chamber proved that no combustion had occurred before release of oxygen from the metal oxide resource.

2015 *J. Micromech. Microeng.* **25** 104006

Wafer level fabrication of single cell dispenser chips with integrated electrodes for particle detection

Jonas Schoendube, Azmi Yusof, Kiril Kalkandjiev, Roland Zengerle and Peter Koltay

Abstract

This work presents the microfabrication and experimental evaluation of a dispenser chip, designed for isolation and printing of single cells by combining impedance sensing and drop-on-demand dispensing. The dispenser chip features 50 × 55 µm (width × height) microchannels, a droplet generator and microelectrodes for impedance measurements. The chip is fabricated by sandwiching a dry film photopolymer (TMMF) between a silicon and a Pyrex wafer. TMMF has been used to define microfluidic channels, to serve as low temperature (75 °C) bonding adhesive and as etch mask during 300 µm deep HF etching of the Pyrex wafer. Due to the novel fabrication technology involving the dry film resist, it became possible to fabricate facing electrodes at the top and bottom of the channel and to apply electrical impedance sensing for particle detection with improved performance. The presented microchip is capable of dispensing liquid and detecting microparticles via impedance measurement. Single polystyrene particles of 10 µm size could be detected with a mean signal amplitude of 0.39 ± 0.13 V (n = 439) at particle velocities of up to 9.6 mm s^{-1} inside the chip.

2015 *J. Micromech. Microeng.* **25** 025008

Flip-chip integration of Si bare dies on polymeric substrates at low temperature using ICA vias made in dry film photoresist

Andrés Vásquez Quintero, Danick Briand and Nico F de Rooij

Abstract

In this paper, a low temperature flip-chip integration technique for Si bare dies is demonstrated on flexible PET substrates with screen-printed circuits. The proposed technique is based on patterned blind vias in dry film photoresist (DP) filled with isotropic conductive adhesive (ICA). The DP material serves to define the vias, to confine the ICA paste (80 µm-wide and potentially 25 µm-wide vias), as an adhesion layer to improve the mechanical robustness of the assembly, and to protect additional circuitry on the substrate. The technique is demonstrated using gold-bumped daisy chain chips (DCCs), with electrical vias resistances in the order to hundreds of milliohms, and peel/shear adhesion strengths of 0.7 N mm^{-1} and 3.2 MPa, respectively, (i.e. at 1.2 MPa of bonding pressure). Finally, the mechanical robustness to bending forces was optimized through flexural mechanics models by placing the neutral plane at the DCC/DP adhesive interface. The optimization was performed by reducing the Si thickness from 400 to 37 µm, and resulted in highly robust integrated assemblies withstanding 10 000 cycles of dynamic bending at 40 mm of radius, with relative changes in vias resistance lower than 20%. In addition, the electrical vias resistance and adhesion strengths were compared to samples integrated with anisotropic conductive adhesives (ACAs). Besides the low temperature and high integration resolution, the proposed method is compatible with large area fabrication and multilayer architectures on foil.

2015 *J. Micromech. Microeng.* **25** 045013

Mould insert fabrication of a single-mode fibre connector alignment structure optimized by justified partial metallization

Markus Wissmann, Nicole Barié, Markus Guttmann, Marc Schneider, Alexander Kolew, Heino Besser, Wilhelm Pfleging, Andreas Hofmann, Jürgen Van Erps, Stefano Beri and Jan Watté

Abstract

For mass production of multiscale-optical components, microstructured moulding tools are needed. Metal tools are used for hot embossing or injection moulding of microcomponents made of a thermoplastic polymer. Microstructures with extremely tight specifications, e.g. low side wall roughness and high aspect ratios are generally made by lithographic procedures such as x-ray lithography or deep proton writing. However, these processes are unsuitable for low-cost mass production. An alternative manufacturing method of moulding tools has been developed at the Karlsruhe Institute of Technology (KIT). This article describes a mould insert fabrication and a new replication process for self-centring fibre alignment structures for low loss field installable single-mode fibre connectors, developed and fabricated by the Vrije Universiteit Brussel (VUB) in collaboration with TE Connectivity. These components are to be used in fibre-to-the-home networks and support the deployment and maintenance of fibre optic links. The special feature of this particular fibre connector is a self-centring fibre alignment, achieved by means of a through hole with deflectable cantilevers acting as micro-springs. The particular challenge is the electroforming of through holes with a centre hole diameter smaller than 125 µm. The fibre connector structure is prototyped by deep proton writing in polymethylmethacrylate and used as a sacrificial part. Using joining, physical vapour deposition and electroforming technology, a negative copy of the prototyped connector is transferred into nickel to be used as a moulding tool. The benefits of this replication technique are a rapid and economical fabrication of moulding tools with high-precision microstructures and a long tool life. With these moulding tools low-cost mass production is possible. We present the manufacturing chain we have established. Each individual manufacturing step of the mould insert fabrication will be shown in this report. The process reliability and suitability for mass production was tested by hot embossing.

2015 *J. Micromech. Microeng.* **25** 035008

Electroformed four-spring self-centring fibre alignment structure in nickel.

PolyMUMPs MEMS device to measure mechanical stiffness of single cells in aqueous media

S Warnat, H King, C Forbrigger and T Hubbard

Abstract

A method of experimentally determining the mechanical stiffness of single cells by using differential displacement measurements in a two stage spring system is presented. The spring system consists of a known MEMS reference spring and an unknown cellular stiffness: the ratio of displacements is related to the ratio of stiffness. A polyMUMPs implementation for aqueous media is presented and displacement measurements made from optical microphotographs using a FFT based displacement method with a repeatability of ~20 nm. The approach was first validated on a MEMS two stage spring system of known stiffness. The measured stiffness ratios of control structures (i) MEMS spring systems and (ii) polystyrene microspheres were found to agree with theoretical values. Mechanical tests were then performed on *Saccharomyces cerevisiae* (Baker's yeast) in aqueous media. Cells were placed (using a micropipette) inside MEMS measuring structures and compressed between two jaws using an electrostatic actuator and displacements measured. Tested cells showed stiffness values between 5.4 and 8.4 N m^{-1} with an uncertainty of 11%. In addition, non-viable cells were tested by exposing viable cells to methanol. The resultant mean cell stiffness dropped by factor of 3× and an explicit discrimination between viable and non-viable cells based on mechanical stiffness was seen.

2015 *J. Micromech. Microeng.* **25** 025011

Internal passivation of Al-based microchannel devices by electrochemical anodization

Paul J Hymel, D S Guan, Yang Mu, W J Meng and Andrew C Meng

Abstract

Metal-based microchannel devices have wide-ranging applications. We report here a method to electrochemically anodize the internal surfaces of Al microchannels, with the purpose of forming a uniform and dense anodic aluminum oxide (AAO) layer on microchannel internal surfaces for chemical passivation and corrosion resistance. A pulsed electrolyte flow was utilized to emulate conventional anodization processes while replenishing depleted ionic species within Al microtubes and microchannels. After anodization, the AAO film was sealed in hot water to close the nanopores. Focused ion beam (FIB) sectioning, scanning electron microscopy (SEM), and energy dispersive spectroscopy (EDS) were utilized to characterize the AAO morphology and composition. Potentiodynamic polarization corrosion testing of anodized Al microtube half-sections in a NaCl solution showed an order of magnitude decrease in anodic corrosion current when compared to an unanodized tube. The surface passivation process was repeated for Al-based microchannel heat exchangers. A corrosion testing method based on the anodization process showed higher resistance to ion transport through the anodized specimens than unanodized specimens, thus verifying the internal anodization and sealing process as a viable method for surface passivation of Al microchannel devices.

2015 *J. Micromech. Microeng.* **25** 027003

A fabrication process for the monolithic integration of magnetoelastic actuators and silicon sensors

Jun Tang, Scott R Green and Yogesh B Gianchandani

Abstract

This paper describes a microfabrication process that accommodates the design considerations of wirelessly actuated magnetoelastic traveling wave and standing wave motors that are integrated with capacitive position sensors on a silicon substrate. The process—which incorporates AuIn eutectic bonding, multiple deep reactive ion etching steps, and metal electrode deposition and etching—addresses the challenges of magnetoelastic layer attachment, multi-layer structures, and robust electrode isolation. Measurements of successfully fabricated devices show that the typical resonant frequencies of the clockwise and counterclockwise modes for the standing wave stators existed at 12.1 and 22.4 kHz with 0.44 μm and 0.4 μm out-of-plane amplitudes, respectively, when a ≈2 Oe amplitude ac magnetic field and a ≈6.5 Oe dc magnetic bias field were applied. For the as-fabricated traveling wave motors, two desired mode shapes with π/2 spatial phase shift existed at typical frequencies of 28.4 and 29.9 kHz, with typical out-of-plane amplitudes of 74 and 70 nm, respectively, when a ≈6 Oe amplitude ac magnetic field and a ≈3 Oe dc magnetic bias field were applied. The frequencies were tuned with added mass, resulting in a shift to 28.37 and 28.33 kHz with out-of-plane amplitudes of 80 and 60 nm for the two modes, respectively. After tuning, a traveling wave with a continuous direction of propagation was successfully demonstrated. The capacitive position sensing scheme showed a sensitivity of ≈0.5 pF per degree over 8°.

2015 *J. Micromech. Microeng.* **25** 045001

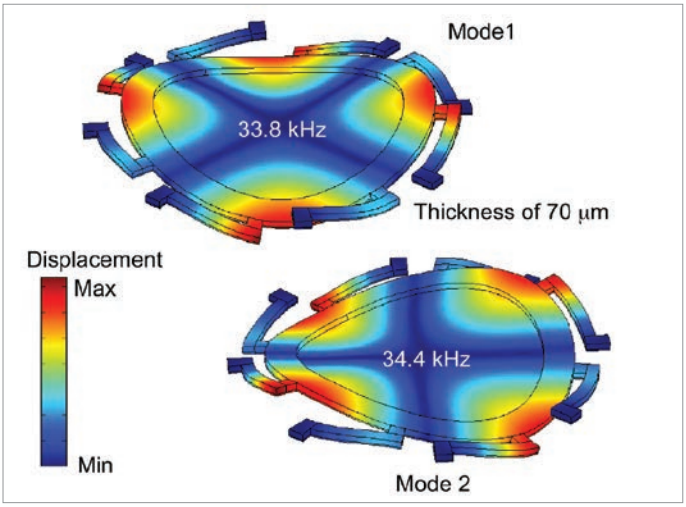

FEA simulations of eigenfrequencies for a standing wave stator.

Plasmonic lithography for fabricating nanoimprint masters with multi-scale patterns

Howon Jung, Seok Kim, Dandan Han, Jinhee Jang, Seonghyeon Oh, Jun-Hyuk Choi, Eung-Sug Lee and Jae W Hahn

Abstract

We successfully demonstrate the practical application of plasmonic lithography to fabricate nanoimprint masters. Using the properties of a non-propagating near-field, we achieve high-speed multi-scale patterning with different exposure time during the scanning. We modulate the width of the line patterns using a pulse light source with different duty cycles during the scanning of the probe. For practical application in plasmonic lithography, we apply a deep reactive ion etching process to transfer an arbitrary fluidic channel into a silicon substrate and fabricate a high-aspect-ratio imprint master. Subsequently, we carry out the imprint process to replicate the fluidic channel with an aspect ratio of 7.2. For pattern width below 100 nm, we adopt a three-layer structure of photoresist, hard layer, and polymer to record the near field and form a hard mask and transfer mask. Using the multilayer structure, we fabricate high-resolution nanoimprint masters in a silicon substrate with an aspect ratio greater than 1.

2015 *J. Micromech. Microeng.* **25** 055004

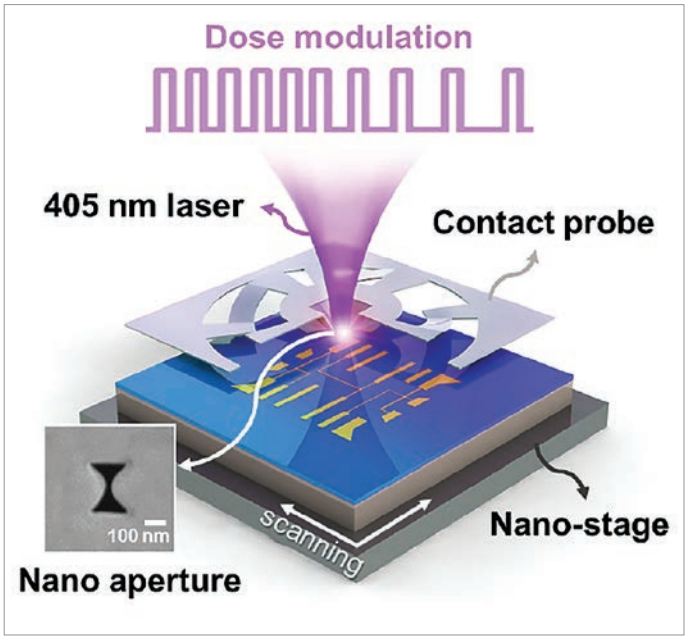

Schematic of the maskless plasmonic lithography system.

Flexible structured high-frequency film bulk acoustic resonator for flexible wireless electronics

Changjian Zhou, Yi Shu, Yi Yang, Hao Jin, Shu-Rong Dong, Mansun Chan and Tian-Ling Ren

Abstract

Flexible electronics have inspired many novel and very important applications in recent years and various flexible electronic devices such as diodes, transistors, circuits, sensors, and radiofrequency (RF) passive devices including antennas and inductors have been reported. However, the lack of a high-performance RF resonator is one of the key bottlenecks to implement flexible wireless electronics. In this study, for the first time, a novel ultra-flexible structured film bulk acoustic resonator (FBAR) is proposed. The flexible FBAR is fabricated on a flexible polyimide substrate using piezoelectric thin film aluminum nitride (AlN) for acoustic wave excitation. Both the shear wave and longitudinal wave can be excited under the surface interdigital electrodes configuration we proposed. In the case of the thickness extension mode, a flexible resonator with a working frequency as high as of 5.2325 GHz has been realized. The resonators stay fully functional under bending status and after repeated bending and re-flattening operations. This flexible high-frequency resonator will serve as a key building block for the future flexible wireless electronics, greatly expanding the application scope of flexible electronics.

2015 *J. Micromech. Microeng.* **25** 055003

Modeling and experimental verification of thermally induced residual stress in RF-MEMS

Aurelio Somà and Muhammad Mubasher Saleem

Abstract

Electrostatically actuated radio frequency microelectromechanical systems (RF-MEMS) generally consist of microcantilevers and clamped–clamped microbeams. The presence of residual stress in these microstructures affects the static and dynamic behavior of the device. In this study, nonlinear finite element method (FEM) modeling and the experimental validation of residual stress induced in the clamped–clamped microbeams and the symmetric toggle RF-MEMS switch (STS) is presented. The formation of residual stress due to plastic deformation during the thermal loading-unloading cycle in the plasma etching step of the microfabrication process is explained and modeled using the Bauschinger effect. The difference between the designed and the measured natural frequency and pull-in voltage values for the clamped–clamped microbeams is explained by the presence of the nonhomogenous tensile residual stress. For the STS switch specimens, three-dimensional (3D) FEM models are developed and the initial deflection at zero bias voltage, observed during the optical profile measurements, is explained by the residual stress developed during the plasma etching step. The simulated residual stress due to the plastic deformation is included in the STS models to obtain the switch pull-in voltage. At the end of the simulation process, a good correspondence is obtained between the FEM model results and the experimental measurements for both the clamped–clamped microbeams and the STS switch specimens.

2015 *J. Micromech. Microeng.* **25** 055007

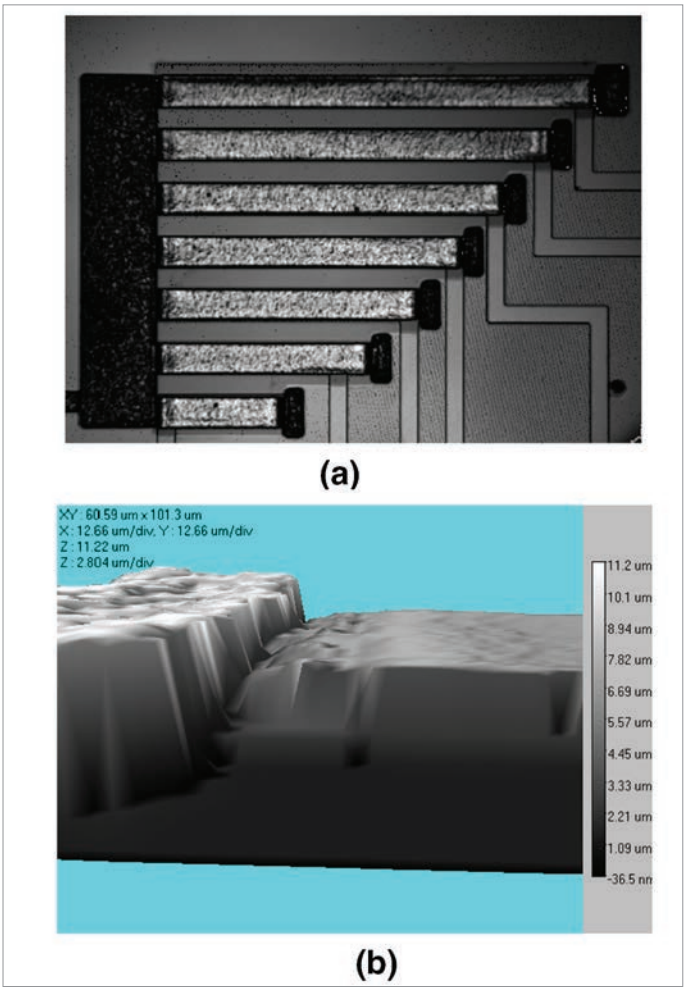

(a) Optical image of a microbeam test structure array, (b) 3D image of the anchor region.

Design and modeling of a light powered biomimicry micropump

Tsun-kay Jackie Sze, Jin Liu and Prashanta Dutta

Abstract

The design of compact micropumps to provide steady flow has been an on-going challenge in the field of microfluidics. In this work, a novel micropump concept is introduced utilizing bacteriorhodopsin and sugar transporter proteins. The micropump utilizes light energy to activate the transporter proteins, which create an osmotic pressure gradient and drive the fluid flow. The capability of the bio inspired micropump is demonstrated using a quasi 1D numerical model, where the contributions of bacteriorhodopsin and sugar transporter proteins are taken care of by appropriate flux boundary conditions in the flow channel. Proton flux created by the bacteriorhodopsin proteins is compared with experimental results to obtain the appropriate working conditions of the proteins. To identify the pumping capability, we also investigate the influences of several key parameters, such as the membrane fraction of transporter proteins, membrane proton permeability and the presence of light. Our results show that there is a wide bacteriorhodopsin membrane fraction range (from 0.2 to 10%) at which fluid flow stays nearly at its maximum value. Numerical results also indicate that lipid membranes with low proton permeability can effectively control the light source as a method to turn on/off fluid flow. This capability allows the micropump to be activated and shut off remotely without bulky support equipment. In comparison with existing micropumps, this pump generates higher pressures than mechanical pumps. It can produce peak fluid flow and shutoff head comparable to other non-mechanical pumps.

2015 *J. Micromech. Microeng.* **25** 065009

Perturbation-induced droplets for manipulating droplet structure and configuration in microfluidics

Jingmei Li, Nitesh Mittal, Sze Yi Mak, Yang Song and Ho Cheung Shum

Abstract

In this work, we mechanically perturb a liquid-in-liquid jet to manipulate the size and structure of the droplets formed from break-up of the jet. The induced break-up is relatively insensitive to fluctuations in the surrounding fluid flow. When the amplitude of perturbations is large and the interfacial tension of the liquid–liquid system is low, the size of the droplets can be precisely tuned by controlling the rate at which the liquid exits the tip of the dispensing nozzle through the frequency of perturbation. When applied to microfluidic devices with the appropriate geometry, our perturbation-induced droplet approach offers a strategy to manipulating droplet structures. We demonstrate that by varying the imposed perturbation frequency and phase lag, the structure of the multi-compartmental drops and the configuration of the resultant drops in the same flow condition can be manipulated. Moreover, after careful treatment of the wettability of the devices, we show that the structure of the droplets can be precisely controlled to change from single emulsion to double emulsion within the same device. The perturbation-induced droplet generation represents a new paradigm in the engineering of droplets, enhancing current droplet-based technologies for applications ranging from particle fabrication to confined micro-reactions.

2015 *J. Micromech. Microeng.* **25** 084009

On-chip aqueous two-phase system (ATPS) formation, consequential self-mixing, and their influence on drop-to-drop aqueous two-phase extraction kinetics

Pavithra A L Wijethunga and Hyejin Moon

Abstract

Aqueous two-phase systems (ATPSs) allow an advantageous aqueous two-phase extraction process (ATPE), a special type of liquid–liquid extraction. Compared with conventional liquid–liquid extraction using aqueous/organic extraction media, ATPE is known to provide relatively easy mass transfer and a gentle environment for biological separation applications. Considering the recent interest in microscale ATPE, we aimed to study (i) the potential of preparing ATPS droplets on a digital microfluidic device, and (ii) the influence of the fluidic dynamics created during the formation of ATPS, with the goal of enhancing on-chip ATPE process. On-chip ATPS formation was evaluated by preparing a series of ATPSs on electrowetting on dielectric digital microfluidic chips and comparing their characteristics with the same ATPSs prepared at macroscale using conventional procedures. An enhanced on-chip drop-to-drop ATPE process was achieved by incorporating a self-mixing condition created during ATPSformation. Results indicate a successful on-chip ATPS preparation as well as enhanced extraction performance by self-mixing in the absence of forced mixing. Findings of this research suggest an alternative, simple, yet adequate technique to provide mixing for on-chip applications, such as sample preparation in portable microfluidics, for which it is unfavorable to implement complicated mixing sequences or complex device geometries.

2015 *J. Micromech. Microeng.* **25** 094002

Monolithic transparent 3D dielectrophoretic micro-actuator fabricated by femtosecond laser

Tao Yang and Yves Bellouard

Abstract

We demonstrate a three-dimensional (3D) monolithic micro-actuator fabricated by non-ablative femtosecond laser micromachining and subsequent chemical etching. The actuating principle is based on dielectrophoresis. An analytical modeling of this actuation scheme is conducted, which is capable of performance prediction, parameter optimization and instability analysis. Static and dynamic characterizations are experimentally verified. An actuation range of 30 µm is well attainable; resonances are captured with an evaluated quality factor of 40 (measured in air) and a bandwidth of 5 Hz for the primary vertical resonance of 200 Hz. A settling time of 200 ms in transient response indicates the damping properties of such actuation scheme. This actuation principle suppresses the need for electrodes on the mobile, non-conductive component and is particularly interesting for moving transparent elements. Thanks to the flexibility of the manufacturing process, it can be coupled to other functionalities within monolithic transparent micro-electro-mechanical systems (MEMS) for applications like tunable optical couplers.

2015 *J. Micromech. Microeng.* **25** 105009

A simple approach for the fabrication of 3D microelectrodes for impedimetric sensing

Mustafa Tahsin Guler, Ismail Bilican, Sedat Agan and Caglar Elbuken

Abstract

In this paper, we present a very simple method to fabricate three-dimensional (3D) microelectrodes integrated with microfluidic devices. We form the electrodes by etching a microwire placed across a microchannel. For precise control of the electrode spacing, we employ a hydrodynamic focusing microfluidic device and control the width of the etching solution stream. The focused widths of the etchant solution and the etching time determine the gap formed between the electrodes. Using the same microfluidic device, we can fabricate integrated 3D electrodes with different electrode gaps. We have demonstrated the functionality of these electrodes using an impedimetric particle counting setup. Using 3D microelectrodes with a diameter of 25 µm, we have detected 6 µm-diameter polystyrene beads in a buffer solution as well as erythrocytes in a PBS solution. We study the effect of electrode spacing on the signal-to-noise ratio of the impedance signal and we demonstrate that the smaller the electrode spacing the higher the signal obtained from a single microparticle. The sample stream is introduced to the system using the same hydrodynamic focusing device, which ensures the alignment of the sample in between the electrodes. Utilising a 3D hydrodynamic focusing approach, we force all the particles to go through the sensing region of the electrodes. This fabrication scheme not only provides a very low-cost and easy method for rapid prototyping, but which can also be used for applications requiring 3D electric field focused through a narrow section of the microchannel.

2015 *J. Micromech. Microeng.* **25** 095019

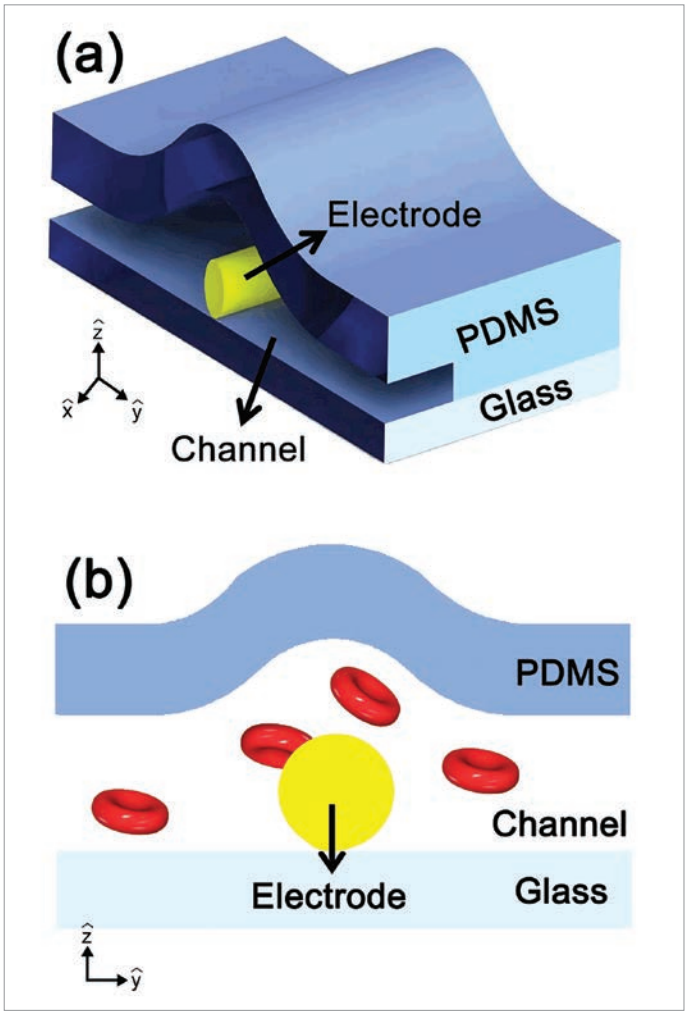

Schematics of a 3D microwire sensor.

Temperature dependent performance of piezoelectric MEMS resonators for viscosity and density determination of liquids

G Pfusterschmied, M Kucera, E Wistrela, T Manzaneque, V Ruiz-Díez, J L Sánchez-Rojas, A Bittner and U Schmid

Abstract

It is the objective of this paper to report on the performance of piezoelectric MEMS resonators for viscosity and density measurements at elevated temperatures. A custom-built temperature controlled measurement setup is designed for fluid temperatures up to 100 °C. Piezoelectric single-side clamped resonators are fabricated, excited in 2nd order of the roof tile-shaped mode (13-mode) and exposed to several liquids (i.e. D5, N10, N35, PAO8, olive oil, ester oil and N100). At the next step, these results are analysed applying a straightforward evaluation model, thus demonstrating that with piezoelectric MEMS resonators the density (i.e. from $\rho_{min} = 785\,kg\,m^{-3}$ to $\rho_{max} = 916\,kg\,m^{-3}$) and viscosity (i.e. from $\mu_{min} = 1.20$ mPa s to $\mu_{max} = 286.36$ mPa s) values of liquids can be precisely determined in a wide range. Compared to standard measurement techniques, the results show for the first parameter a mean deviation of about 1.04% at 100 °C for all the liquids investigated. For the second parameter, the standard evaluation model implies a systematic deviation in viscosity with respect to the calibration being N35 in this study. This inherent lack of strength has a significant influence on the accuracy, especially at 100 °C due to fluids having a viscosity reduced by a factor of 30 for N100 compared to room temperature. This leads to relative deviations of about 23% at 100 °C and indicates the limits of the evaluation model.

2015 *J. Micromech. Microeng.* **25** 105014

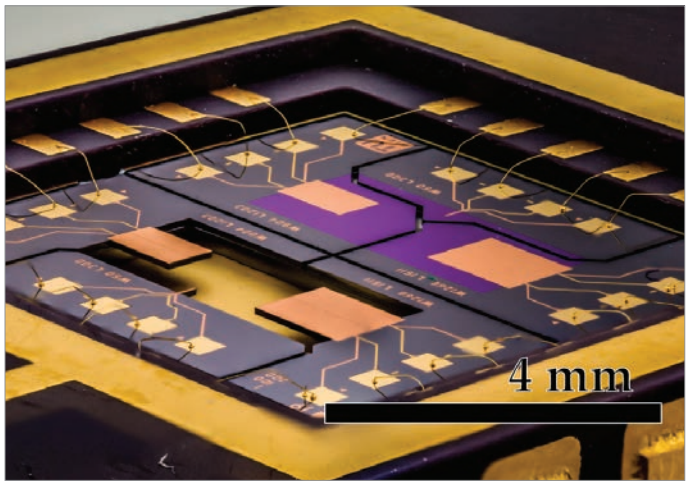

Packaged and bonded MEMS resonant sensor die.

Defective carbon nanotube-silicon heterojunctions for photodetector and chemical sensor with improved responses

Jungwook Choi and Jongbaeg Kim

Abstract

The direct growth and integration of defect-modulated carbon nanotubes (CNTs) on n-type silicon (Si) microstructures for high performance photodetectors and chemiresistive sensors is presented. By devising a Si microspring that is strained by the growth force of the CNTs, a vertical load from the restoring force of the microspring is perpendicularly applied against the growth direction of the CNTs. This vertical load induces the formation of defective structures in the CNTs while the CNT–Si heterojunctions are fabricated. Under the illumination of UV light, photogenerated carriers from both the CNTs and the Si can be separated at the CNT–Si heterojunctions and at the defects in the CNTs before recombination, which contributes to a high photoresponsivity of 262.3 mA W^{-1} and an external quantum efficiency of 91.4%. Moreover, the adsorption of chemical species can be promoted by increasing the defects in the CNTs, thereby improving the sensing responsiveness toward ethanol and NO_2 vapors. Our simple and facile growth of defect-adjusted CNTs on conductive Si microstructures would be beneficial to the scalable, high throughput manufacturing of heterojunctioned devices with tunable properties and functionalities of the CNTs.

2015 *J. Micromech. Microeng.* **25** 115004

IR sensor array using photo-patternable temperature sensitive paint for thermal imaging

T Tsukamoto, M Wang and S Tanaka

Abstract

This paper reports an infrared-to-visible transducer array made of temperature sensitive paint (TSP) for a low-cost thermal imaging application. A novel fabrication process using a photo-patternable temperature sensitive paint (PTSP) combined with an SU-8 transfer method was developed. A PTSP microstructure as small as 2 µm was successfully patterned by the normal photolithography process, and sensitivity as high as −0.5%/°C was obtained. The proposed method simplifies the fabrication process, and prevents the TSP from plasma-induced damage. A self-suspended structure as small as 70 µm was successfully fabricated with a large-gap of 40 µm from the substrate. The heated object at 250 °C was detectable with a spatial resolution of about 380 µm.

2015 *J. Micromech. Microeng.* **25** 104011

A novel all-elastomer MEMS tactile sensor for high dynamic range shear and normal force sensing

Alexi Charalambides and Sarah Bergbreiter

Abstract

A novel all-elastomer MEMS tactile sensor with high dynamic force range is presented in this work. Conductive elastomeric capacitors formed from electrodes of varying heights enable robust sensing in both shear and normal directions without the need for multi-layered assembly. Sensor geometry has been tailored to maximize shear force sensitivity using multi-physics finite element simulations. A simple molding microfabrication process is presented to rapidly create the sensing skins with electrode gaps of 20 µm and sensor spacing of 3 mm. Shear force resolution was found to be as small as 50 mN and tested up to a range of 2 N (dynamic range of 40:1). Normal force resolution was found to be 190 mN with a tested range of 8 N (dynamic range of 42:1). Single load and multiload tests were conducted and the sensor exhibited intended behavior with low deviations between trials. Spatial tests were conducted on a 2 × 2 sensor array and a spatial resolution of 1.5 mm was found.

2015 *J. Micromech. Microeng.* **25** 095009

Nonhomogeneous morphology and the elastic modulus of aligned carbon nanotube films

Yoonjin Won, Yuan Gao, Roberto Guzman de Villoria, Brian L Wardle, Rong Xiang, Shigeo Maruyama, Thomas W Kenny and Kenneth E Goodson

Abstract

Carbon nanotube (CNT) arrays offer the potential to develop nanostructured materials that leverage their outstanding physical properties. Vertically aligned carbon nanotubes (VACNTs), also named CNT forests, CNT arrays, or CNT turfs, can provide high heat conductivity and sufficient mechanical compliance to accommodate thermal expansion mismatch for use as thermal interface materials (TIMs). This paper reports measurements of the in-plane moduli of vertically aligned, single-walled CNT (SWCNT) and multi-walled CNT (MWCNT) films. The mechanical response of these films is related to the nonhomogeneous morphology of the grown nanotubes, such as entangled nanotubes of a top crust layer, aligned CNTs in the middle region, and CNTs in the bottom layer. To investigate how the entanglements govern the overall mechanical moduli of CNT films, we remove the crust layer consisting of CNT entanglements by etching the CNT films from the top. A microfabricated cantilever technique shows that crust removal reduces the resulting moduli of the etched SWCNT films by as much as 40%, whereas the moduli of the etched MWCNT films do not change significantly, suggesting a minimal crust effect on the film modulus for thick MWCNT films (>90 μm). This improved understanding will allow us to engineer the mechanical moduli of CNT films for TIMs or packaging applications.

2015 *J. Micromech. Microeng.* **25** 115023

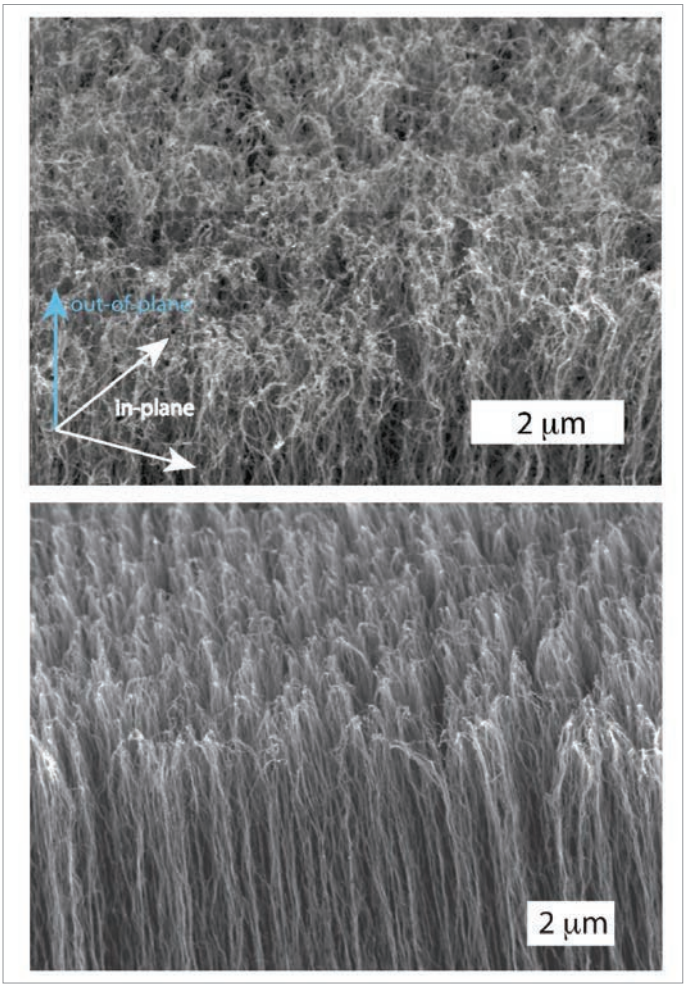

Crust layer of a MWCNT film (top) before and (bottom) after etching.

A CMOS–MEMS arrayed resonant-gate field effect transistor (RGFET) oscillator

Chi-Hang Chin, Ming-Huang Li, Chao-Yu Chen, Yu-Lin Wang and Sheng-Shian Li

Abstract

A high-frequency CMOS–MEMS arrayed resonant-gate field effect transistor (RGFET) fabricated by a standard 0.35 μm 2-poly-4-metal CMOS–MEMS platform is implemented to enable a Pierce-type oscillator. The proposed arrayed RGFET exhibits low motional impedance of only 5 kΩ under a purely capacitive transduction and decent power handling capability. With such features, the implemented oscillator shows impressive phase noise of −117 dBc Hz^{-1} at the far-from-carrier offset (1 MHz). In this work, we design a clamped–clamped beam (CCB) arrayed resonator utilizing a high-velocity mechanical coupling scheme to serve as the resonant-gate array. To achieve a functional arrayed RGFET, a corresponding FET array is directly placed underneath the resonant gate array to convert the motional current on the resonant-gate array into a voltage output with a tunable transconductance gain. To understand the behavior of the proposed device, an equivalent circuit model consisting of the resonant unit and FET is also provided. To verify the effects of the post-CMOS process on device performance, a conventional MOS I_D current measurement is carried out. Finally, a CMOS–MEMS arrayed RGFET oscillator is realized by utilizing a Pierce oscillator architecture, showing decent phase noise performance that benefits from the array design to alleviate the nonlinear effect of the resonant gate.

2015 *J. Micromech. Microeng.* **25** 115025

Tuning magnetofluidic spreading in microchannels

Zhaomeng Wang, V B Varma, Z P Wang and R V Ramanujan

Abstract

Magnetofluidic spreading (MFS) is a phenomenon in which a uniform magnetic field is used to induce spreading of a ferrofluid core cladded by diamagnetic fluidic streams in a three-stream channel. Applications of MFS include micromixing, cell sorting and novel microfluidic lab-on-a-chip design. However, the relative importance of the parameters which govern MFS is still unclear, leading to non-optimal control of MFS. Hence, in this work, the effect of various key parameters on MFS was experimentally and numerically studied. Our multi-physics model, which combines magnetic and fluidic analysis, showed excellent agreement between theory and experiment. It was found that spreading was mainly due to cross-sectional convection induced by magnetic forces, and can be enhanced by tuning various parameters. Smaller flow rate ratio, higher magnetic field, higher core stream or lower cladding stream dynamic viscosity, and larger magnetic particle size can increase MFS. These results can be used to tune magnetofluidic spreading in microchannels.

2015 *J. Micromech. Microeng.* **25** 124001